19th Australasian Fluid Mechanics Conference
Melbourne, Australia
8-11 December 2014

Frequency selection and phase locking during aeroelastic galloping

J. S. Leontini[1], J. Zhao[2], H. G. K. G. Jayatunga[3], D. Lo Jacono[2,4], B. T. Tan[3] and J. Sheridan[2]

[1]Department of Mechanical and Product Design Engineering
Swinburne University of Technology, John St Hawthorn, Victoria 3162, Australia

[2]Fluids Laboratory for Aeronautical and Industrial Research (FLAIR), Department of Mechanical And Aerospace Engineering
Monash University, Wellington Rd Clayton, Victoria 3800, Australia

[3]Malaysia School of Engineering
Monash University Sunway Malaysia, Jalan Universiti, Bandar Sunway, Subang Jaya Selangor, Malaysia

[4]Université de Toulouse; INP; IMFT (Institut de Mécanique des Fluides de Toulouse)
Allée Camille Soula, F-31400 Toulouse, France

Abstract

This paper presents an analysis of the aeroelastic galloping of an elastically mounted square cross section in a free stream. The classic quasi-steady model [1] is used as a starting point. From this, the relevant time scales and dimensionless groups of the problem are derived. The time scale analysis shows that the mechanism of frequency selection by the oscillating system changes for heavy and light bodies. Results from direct numerical simulations are presented and compared against results from the simplified quasi-steady model, showing that the quasi-steady is quantitatively valid for heavy bodies, and at least generally qualitatively valid for light bodies. Results of experiments on light bodies also show this general qualitative agreement. However, there are also regimes of nonlinear interaction between the galloping and vortex shedding that the simplified model cannot capture.

Introduction

Aeroelastic galloping is a classic fluid-structure interaction phenomenon that can occur when a body is immersed in a flow. In its simplest form, the body needs to be long in a direction perpendicular to the flow and have a constant cross section that can have an angle of attack (such a s square beam, but not a circular cylinder), and be elastically mounted and free to move transverse to the direction of the flow. The instability is caused by an interaction between the motion of the body and the aerodynamic forces on the body (hence the term aeroelastic); if a small motion away from the body's equilibrium position transverse to the flow induces mean transverse (lift) forces in that same direction, the equilibrium position is unstable and the body will begin to oscillate.

If the body's transverse velocity is added to the incoming flow velocity in a vector sense, the body will be at a relative angle of attack to the total flow. The mean lift force as a function of the angle of attack can be measured from experiments for the given body, and so the force on the oscillating body can be written as a function of the transverse velocity. Note the reliance on the mean lift force implies that it is assumed that the motion of the body is relatively slow, or quasi-steady. Essentially this means the fluctuations in the lift force due to the vortex shedding in the wake can be ignored. If the body is modelled as a spring-mass-damper system, this process results in a nonlinear ordinary differential equation for the body's transverse motion.

Such a simplified quasi-static model has been developed [1]. For a square cross section can be written as

$$m\ddot{y}+c\dot{y}+ky = \frac{1}{2}\rho U^2 DL\left(a_1\left(\frac{\dot{y}}{U}\right)+a_3\left(\frac{\dot{y}}{U}\right)^3+a_5\left(\frac{\dot{y}}{U}\right)^5+a_7\left(\frac{\dot{y}}{U}\right)^7\right). \quad (1)$$

where m is the mass of the body, y is the body transverse displacement, c is the mechanical damping coefficient, k is the spring stiffness, ρ is the fluid density, U is the freestream velocity, D is the side length of the square, L is the length of the beam, and the coefficients a_n are dimensionless coefficients. The value of these coefficients are determined by fitting a polynomial to data of the lift force as a function of angle of attack (which is proportional to the transverse velocity) from static body experiments or simulations.

Here, the validity of this quasi-steady model is investigated. Results obtained by numerically integrating equation (1) are compared to results from fully-coupled direct numerical simulations of the fluid-structure interaction problem. It is shown that the model predicts the motion of the body quantitatively well for heavy bodies. For light bodies, the match is not as close, however the simplified model still qualitatively captures the essential physics of the problem. Results of experiments show that particular regimes exist where there is strong nonlinear interaction between the galloping and the body motion that cannot be captured by the model, but outside of these regimes the model performs reasonably well.

Methodology

Solution of the quasi-steady model

The quasi-steady model shown in equation (1) is a nonlinear ordianry differential equation for the body displacement. No full analytical solution of this equation exists, however it can be simply integrated numerically. The numerical integration of this equation was performed using the built-in function ODE45 in MATLAB, given the system properties and the coefficients a_n. These coefficients come from fitting a curve to data of lift force as a function of angle of attack from static body experiments or simulations. For the data presented here, static body direct numerical simulations at a Reynolds number $Re = UD/\nu = 200$ where ν is the kinematic viscosity, were conducted.

Direct numerical simulations

The aforementioned static body simulations, as well as the fully-coupled fluid-structure simulations, were performed using a high-order spectral element method. The spatial discretization

was achieved by dividing the compuational domain into quadrilateral elements. Each of these elements was further subdivided using internal points associated with the Gauss-Lobatto-Legendre quadrature points. High-order tensor-product Lagrange polynomials were used as shape and weighting functions to solve the weak form of the incompressible Navier–Stokes equations. The time integration was achieved using a three-way time-splitting scheme, allowing the advection, pressure, and diffusion terms to be integrated separately. For the fluid-structure interaction simulations, the equations were solved in the frame of reference attached to the body resulting in an extra acceleration term. This acceleration term was found by solving the Navier–Stokes equations in conjunction with the equation of motion of the body, a simple spring-mass-damper system. Full details of the spectral-element method can be found [2]. Validation of the code employed here is given in a series of papers [3, 4].

Experiments

Experiments were conducted in a free-surface recirculating water channel, the full details of which are presented in previous papers [5]. The setup consisted of a rigid square-section aliminium tube of side length 24.6mm, hanging vertically mounted on an air bearing system [6]. The immersed length was 620mm, giving an aspect ratio of 25.2. The mass ratio of the system could be varied by adding weights to the mounting system. The motion of the body was measured using a non-contact magnetostrictive linear variable differential transformer (LVDT). The lift and drag forces were also measured simultaneously with the body motion using a two-component force balance based on strain gauges configured in a Wheatstone bridge circuit. Full details of the setup and measurement techniques employed can be found elsewhere [7].

Results and discussion

Relevant time scales and dimensionless groups

For a simple spring-mass-damper, the natural time scale of the system is given by the natural frequency. A similar approach can be taken to the system given in equation (1). If this equation is linearized by removing all the terms on the right-hand side except the first, solving for eigenvalues gives

$$\lambda_{1,2} = -\frac{1}{2}\frac{c-\frac{1}{2}\rho U D L a_1}{m} \pm \frac{1}{2}\sqrt{\left[\frac{c-\frac{1}{2}\rho U D L a_1}{m}\right]^2 - 4\frac{k}{m}}. \tag{2}$$

If it is further assumed that the spring and damping forces are relatively weak compared to the aerodynamic forces, ($k \to 0$ and $c \to 0$) this can be reduced to

$$\lambda = \frac{\frac{1}{2}\rho U D L a_1}{m} = \frac{a_1}{m^*}\frac{U}{D}. \tag{3}$$

where m^* is the ratio of the body mass to the mass of displaced fluid. In this form, λ represents the inverse time scale of the motion of the body due to the "negative damping" effect of the mean aerodynamic force.

Using λ to nondimensionalize time so that $\tau = t(a_1/m^*)(U/D)$, the quasi-steady model of equation (1) can be written as

$$\ddot{Y} + \frac{4\pi^2 m^{*2}}{U^{*2} a_1^2} Y = \left(\frac{1}{2} - \frac{c^* m^*}{a_1}\right)\dot{Y} + a_3\left(\frac{a_1}{m^*}\right)^3 \dot{Y}^3 \ldots \tag{4}$$

The coefficients a_n are functions only of the geometry, and the Reynolds number $Re = UD/\nu$, where ν is the fluid kinematic viscosity. Therefore, for a given body and flow, the body response is a function of three dimensionless parameters: a mass-stiffness parameter, $\Pi_1 = 4\pi^2 m^{*2}/U^{*2}$, a mass-damping parameter, $\Pi_2 = c^* m^*$, and the mass ratio m^*, where $U^* = U/(f_N D)$ is the traditional reduced velocity (f_N is the natural frequency $\sqrt{k/m}/(2\pi)$, and $c^* = cD/mU$ is a nondimensional damping.

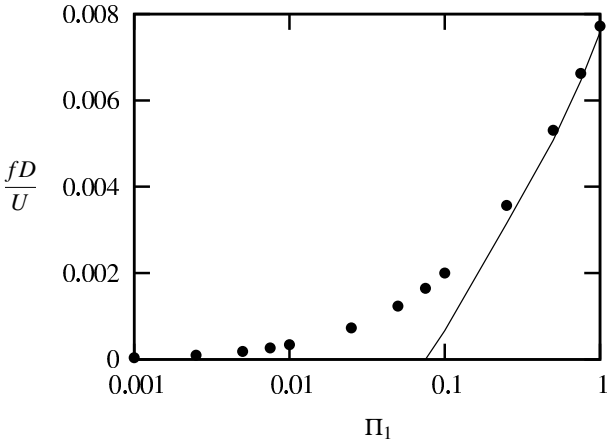

Figure 1: Frequency of the galloping response of a square cylinder, from the quasi-steady model, fluid-structure interaction simulations, and the linearized equation as a function of the mass-stiffness Π_1. (5)

Frequency response regimes

Using the nondimensional parameters defined in section , the eigenvalues of the linearized equation of motion can be written as

$$\frac{\lambda D}{U} = \frac{1}{2}(\Pi_2 - \frac{1}{2}) \pm \sqrt{\Pi_2^2 - \Pi_2 a_1 + \frac{a_1^2}{4} - 4\Pi_1}. \tag{5}$$

While the term under the square root remains negative, the nondimensional eigenvalues $\lambda D/U$ will be complex, and the imaginary component can be used to define a frequency. This is essentially a damped natural frequency that takes into account the negative damping effect of the component of lift force on the body in phase with the body velocity.

However, if the term under the square root is positive, then $\lambda D/U$ represents a non-dimensional growth rate of the body displacement. In this case, no linear frequency is predicted, and any oscillation that occurs must be driven by a nonlinear mechanism.

Inspection of equation (5) shows that for a given value of mass-damping Π_2, there will be a critical value of Π_1 above which the square root term becomes positive and no linear frequency is predicted.

Figure 1 shows the frequency calculated from the numerical solution of equation (4), the frequency calculated from fluid-structure interaction simulations, and the frequency calcuated from the linearized equation (5). The figure shows that the frequency response can essentially be split into two regimes: a linear regime where equation (5) accurately predicts the frequency of oscillation, and a nonlinear regime where equation (5) either predicts no frequency or poorly predicts the frequency of oscillation.

In the nonlinear regime where the influence of stiffness is negligigle, it can be assumed that the body quickly accelerates to a terminal velocity and then continues to move at this velocity until the displacement is so large that the spring forces can no

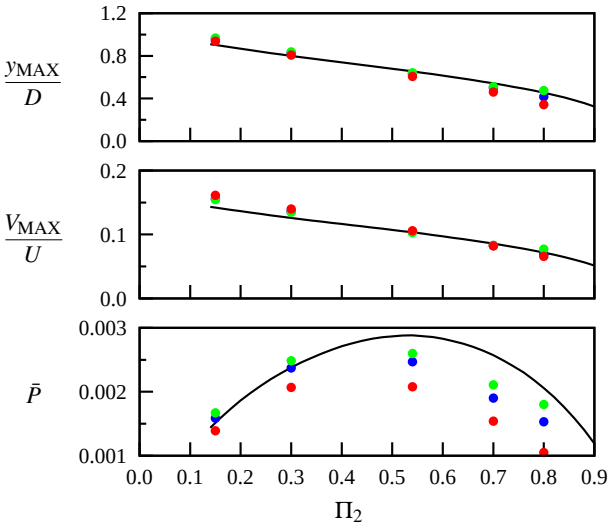

Figure 2: (a) Maximum displacement, (b) maximum velocity and (c) mean power output of the galloping square cylinder as a function of Π_2 for various values of Π_1 calculated from FSI simulations compared to results from the quasi-steady model. • $\Pi_1 = 10$; • $\Pi_1 = 60$; • $\Pi_1 = 250$; (-) quasi-steady model, $\Pi_1 = 10$.

longer be neglected. Assuming small displacements and retaining only up to cubic terms in equation (4), the terminal velocity can be shown to be

$$\dot{Y} = \sqrt{\frac{\Pi_2/a_1 - 1/2}{a_3(a1/m^*)^3}} \qquad (6)$$

with no explicit dependence on Π_1.

Analysis using the quasi-steady model and numerical simulations

The quasi-steady model is based on the assumption that only the long-time forces are important. This assumes the oscillation is much slower than the vortex shedding. A natural question arises; just how well-separated do the oscillation and vortex shedding time scales need to be? How is the accuracy of the quasi-steady model comprimised as these two time scales become close?

To assess this, results from numerically integrating equation (4) are compared to those from direct numerical simulations of the fluid-structure interaction problem. The Reynolds number used is $Re = 200$. Two-dimensional static body simulations were conducted to evaluate the coefficients a_n. The value of $\Pi_1 = 10$, and $m^* = 40$. For these values, the power output of the quasi-steady model is a function of Π_2 only. Two-dimensional fluid-structure interaction (FSI) simulations were then conducted at the same Re, for a series of values of Π_1.

The results show that while the agreement is generally good, the power output predicted by the quasi-steady model is less accurate for lower values of m^*. This is not suprising. As the system mass (and therefore m^*) is decreased, the frequency of the galloping oscillation increases and approaches the vortex shedding frequency. Because of this convergence of time scales, the vortex shedding can interact nonlinearly with the galloping oscillation. The quasi-steady model is based on the assumption that this interaction does not occur, and so at low m^* the underlying assumption of the model is invalid. However, it appears that qualitatively, the quasi-steady model is still able to predict the shape of the curves, indicating that the oscillation phenomena is still similar.

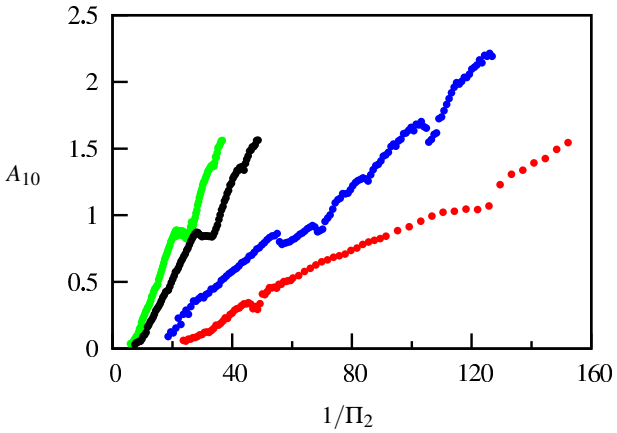

Figure 3: Amplitude of oscillation (represented by A_{10}) as a function $1/\Pi_2$, for a series of small m^*. It is clear that the data do not collapse, indicating a dependence on m^*. Also clear are plateaux, caused by phase locking between the oscillation and a multiple of the vortex shedding. • $m^* = 2.64$; • $m^* = 5$; • $m^* = 11.31$; • $m^* = 15$.

Interaction of galloping and vortex shedding for light bodies

This nonlinear interaction is very well highlighted by experiments on light bodies. Figure 3 shows the amplitude of oscillation (presented as A_{10}, the amplitude exceeded for 10% of the time) as a function of $1/\Pi_2$ for four values of m^*. The data are plotted against $1/\Pi_2$ as this is proportional to the parameter used in classic studies [1] to present data from high-m^* experiments.

Is is clear that the data do not collapse, indicating that there is a dependence on m^* when m^* is low. Efforts to collapse the data in a simple way such as plotting the data as a function of c^* (or Π_2/m^*) have not been successful. An reasonable *ad-hoc* scaling can be found by multiplying $1/\Pi_2$ by an arbitrary factor for each m^* data set, however even then the collapse is not perfect.

The main difficulty for any collapse is the appearance of a series of plateaux or steps in each of the data sets. Focussing on the $m^* = 2.64$ data set in figure 3, there is first a small step around $1/\Pi_2 = 50$, a second around $1/\Pi_2 = 120$, and a third around $1/\Pi_2 = 180$. These steps are caused by nonlinear synchronization between the galloping oscillation and an odd-integer multiple of the vortex shedding. In the first step, there is one vortex shedding cycle per oscillation cycle, in the second there is three vortex shedding cycles per oscillation cycle, etc. A full explanation of these cycles is presented elsewhere [7].

However, outside of these steps, the amplitude appears to increase essentially linearly with $1/\Pi_2$, similar in fashion to the high-m^* data of classic studies [1] and that predicted by the quasi-steady model.

Conclusions

A timescale analysis has been undertaken of aeroelastic galloping of a square cross section, and the dimensionless groups derived used to present data from a classic quasi-steady model, fully-coupled fluid-structure interaction simulations, and experiments. The comparison shows that when the mass of the system is high, the response of the body is governed by a single parameter which is proportional to the product of mass and damping. At low masses however, the response is also a function of the mass ratio, apparently due to interaction between

the galloping oscillation and the vortex shedding. Even though this interaction strictly invalidates the quasi-steady model, this model still appears to at least qualitatively represent the essential physics of the oscillation.

Acknowledgements

The authors acknowledge the financial support of the Australian Research Council through Discovery Project grant DP110102141, and the provision of computational resources and expertise of the Monash University e-research centre, and the National Computational Infrastructure (NCI).

References

[1] Parkinson, G.V. and Smith, J.D., The square prism as an aeroelastic non-linear oscillator, *Quart. Journ. Mech. and Applied Math.*, **17(2)**, 1964, 225–239.

[2] Karniadakis, G.Em. and Sherwin, S., *Spectral/hp element methods for computational fluid dynamics*, Oxford University, 2005.

[3] Thompson, M.C., Hourigan, K., Cheung, A. and Leweke, T., Hydrodynamics of a particle impact on a wall, *App. Math. Model.*, **30(11)**, 2006, 1356–1369.

[4] Leontini, J.S., Stewart, B.E., Thompson, M.C., and Hourigan, K., Predicting vortex-induced vibration from driven oscillation results, *App. Math. Model.*, **30**, 2005, 1096–1102.

[5] Sherry, M., Lo Jacono, D. and Sheridan, J., An experimental investigation of the recirculation zone formed downstream of a forward facing step, *J. Wind Engng. Ind. Aerodyn.*, **98(12)**, 888–894.

[6] Nemes, A., Zhao, J., Lo Jacono, D. and Sheridan, J., The interaction between flow-induced vibration mechanisms of a square cylinder with varying angles of attack, *J. Fluid Mech.*,**710**, 102–130.

[7] Zhao, J., Leontini, J.S., Lo Jacono, D. and Sheridan, J., Fluid-structure interaction of a square cylinder at different angles of attack, *J. Fluid Mech.*, **747**, 688–721.